Microwave V–I Transmission Matrix Formalism for the Analysis of Photonic Circuits: Application to Fiber Bragg Gratings

José Capmany, *Senior Member, IEEE, Fellow, OSA*, Miguel A. Muriel, *Senior Member, IEEE, Member, OSA*, Salvador Sales, *Senior Member, IEEE*, Juan José Rubio, and Daniel Pastor, *Member, IEEE*

***Abstract*—We propose the use of V–I matrices well known in microwave engineering to the analysis of photonic devices, especially those based on multilayer dielectrics. As an application we present a novel fast effective index method for the analysis of fiber Bragg gratings based on the use of V–I transmission matrices. It combines the exactitude of traditional effective index methods and the speed of coupled-mode methods.**

***Index Terms*—Fiber Bragg gratings (FBGs), microwave engineering, photonic devices.**

I. Introduction

MICROWAVE photonics has been defined as a research area dealing with the study of optoelectronic devices and systems processing at microwave rates and with the use of optoelectronic devices and systems for signal handling in microwave systems [1]. Indeed this definition is consequent with the fact that the unique properties of photonic components in terms of bandwidth and low losses can be advantageously exploited to process microwave signals. The interested reader can find a great number of examples in the literature [1]. This beneficial relationship between microwave and photonics engineering can, however, be exploited in the reverse direction as well. Techniques previously developed in microwave engineering can be exploited to solve in an efficient way problems dealing with the design of photonic devices. In this context, there is a rich tradition in microwave engineering related with the development of matrix methods to model circuits and devices [2]. One of these methods is the well-known V–I, ABCD, image parameter or transmission matrix, which is frequently used in the solution of transmission line problems but is relatively unknown to the photonics engineer.

The V–I matrix has the following advantage: since the matrix represents the tangential electric and magnetic fields, transmission through a dielectric discontinuity is expressed by the unity matrix. Therefore, if the V–I matrix is employed to model photonic devices and circuits, no impedance-matching matrices are required for dielectric transitions. This is in contrast to the well-known transfer matrix approach, frequently employed in the modeling of photonic components, where impedance-matching matrices have to be defined for each dielectric discontinuity.

The purpose of this paper is twofold. First, it aims to present the properties of the V–I matrix to the photonics engineering community, outlining its potential for application to the analysis of optical components and devices. Secondly, it provides a specific demonstration of these benefits by developing a novel matrix method for the analysis of fiber Bragg gratings (FBGs) with unique characteristics in terms of precision and computation time. This paper is organized as follows. Section II presents and refreshes the concepts and basic cascading rules of both the transfer matrix (TM) and the transmission matrix (V–I) and provides the relationship between both of them. It is also shown that the V-I matrix for the transition between two dielectrics is the unity matrix. The section is finished with the derivation of the field reflection and transmission coefficients of a device from the knowledge of its overall ABCD matrix.

Section III is devoted to the application of V–I matrices to the analysis of photonic devices in general and FBGs in particular. These are photonic devices based on the periodic or quasi-periodic change of the refractive index along the direction of propagation. We develop a novel and very fast method for the analysis of FBGs based on the V–I formalism, which has an equivalent accuracy to that provided by effective index methods. In Section IV, we present the results obtained by applying the method presented in Section III and its comparison to those based on the solution of coupled-mode equations (CMEs). We show that the V–I formalism is applicable to the solution of any kind of uniform, aperiodic, or sampled FBG and that its computation time is independent of the grating refractive index profile but rather is a function of the grating length and the number of wavelength samples required to represent the spectral variation of its transmission and reflection coefficients. Furthermore, results obtained by using the V–I formalism are compared to those obtained by CME showing almost equivalent computation time while having higher exactitude. Section V presents the summary, conclusions, and future areas of applications.

II. Transmission and Transfer Matrices

We briefly present the main features of transfer and transmission matrices in the description of photonic components showing their main properties and their relationship. We then calculate the transmission matrices of some basic elements that will be employed in Section III.

Manuscript received May 1, 2003; revised September 18, 2003. This work was supported by Spanish CICYT under Projects TIC-2001-3061 and TIC-2001-2869 and EU Projects IST-2001-37435 LABELS and IST-2001-30752 OFFSOHO.

J. Capmany, S. Sales, J. J. Rubio, and D. Pastor are with the IMCO2 Research Institute, Universidad Politécnica de Valencia, 46022 Valencia, Spain.

M. A. Muriel is with the ETSI Telecomunicación, Universidad Politécnica de Madrid, 28040 Madrid, Spain.

Digital Object Identifier 10.1109/JLT.2003.819797

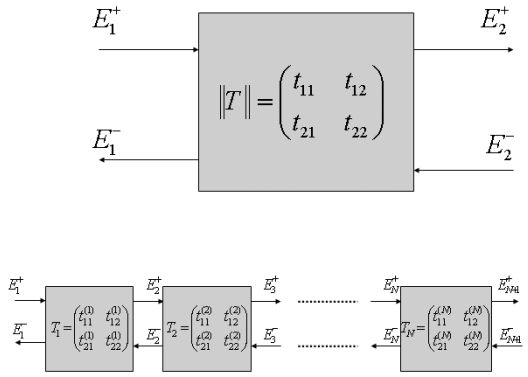

Fig. 1. (a) Box representation of a given photonic device with the forward E_i^+ and backward E_i^- propagating fields at the left and right reference planes for the definition of the transfer matrix. (b) Characterization of complex devices composed of the cascade of elementary components for which the individual transfer matrices are known.

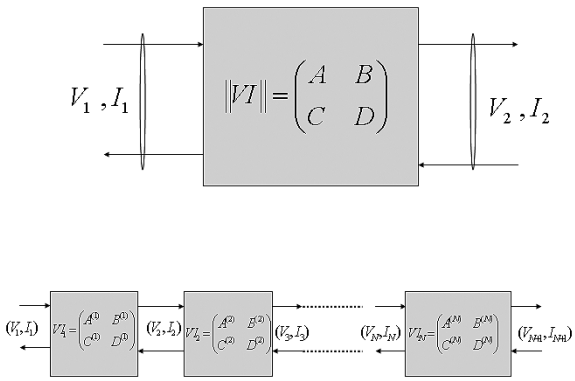

Fig. 2. (a) Box representation of a given photonic device with the tangential transverse electric V and magnetic I fields at the left and right reference planes for the definition of the transmission matrix. (b) Characterization of complex devices composed of the cascade of elementary components for which the individual transmission matrices are known.

A. Basic Definitions and Relationships

In the analysis of photonic components and devices, it is customary to employ the transfer matrix [2], [3]. This formalism can be understood by observing the upper part of Fig. 1. There we show a box representation of a given photonic device with the forward E_i^+ and backward E_i^- propagating fields at the left and right reference planes ($i = 1$ and 2, respectively). The transfer matrix of the device relates those fields in the following way:

$$\begin{pmatrix} E_1^+ \\ E_i^- \end{pmatrix} = \begin{pmatrix} t_{11} & t_{12} \\ t_{21} & t_{22} \end{pmatrix} \cdot \begin{pmatrix} E_2^+ \\ E_2^- \end{pmatrix} = \|T\| \cdot \begin{pmatrix} E_2^+ \\ E_2^- \end{pmatrix}. \quad (1)$$

There are two main reasons why transfer matrices are widely employed in the analysis of photonic components. First, it allows for the straightforward characterization of complex devices composed of the cascade of elementary components for which the individual transfer matrices are known, as shown in the lower part of Fig. 1. In this case, considering (1), it is straightforward to show that

$$\begin{aligned} \begin{pmatrix} E_1^+ \\ E_1^- \end{pmatrix} &= \begin{pmatrix} t_{11}^{(1)} & t_{12}^{(1)} \\ t_{21}^{(1)} & t_{22}^{(1)} \end{pmatrix} \cdot \begin{pmatrix} E_2^+ \\ E_2^- \end{pmatrix} \\ &= \begin{pmatrix} t_{11}^{(1)} & t_{12}^{(1)} \\ t_{21}^{(1)} & t_{22}^{(1)} \end{pmatrix} \begin{pmatrix} t_{11}^{(2)} & t_{12}^{(2)} \\ t_{21}^{(2)} & t_{22}^{(2)} \end{pmatrix} \cdot \begin{pmatrix} E_3^+ \\ E_3^- \end{pmatrix} = \cdots \\ &= \begin{pmatrix} t_{11}^{(1)} & t_{12}^{(1)} \\ t_{21}^{(1)} & t_{22}^{(1)} \end{pmatrix} \cdot \begin{pmatrix} t_{11}^{(2)} & t_{12}^{(2)} \\ t_{21}^{(2)} & t_{22}^{(2)} \end{pmatrix} \cdots \\ &\quad \begin{pmatrix} t_{11}^{(N)} & t_{12}^{(N)} \\ t_{21}^{(N)} & t_{22}^{(N)} \end{pmatrix} \begin{pmatrix} E_{N+1}^+ \\ E_{N+1}^- \end{pmatrix} \\ &= \left[\prod_{j=1}^{N} \|T_j\| \right] \cdot \begin{pmatrix} E_{N+1}^+ \\ E_{N+1}^- \end{pmatrix}. \end{aligned} \quad (2)$$

Equation (2) is the cascade rule for transfer matrices, which states that the overall transfer matrix of a cascade of N elements is the product of the transfer matrices of each element taken form the leftmost to the rightmost element.

The second reason is that the transfer functions for the reflected and transmitted fields in the device are directly obtained once the transfer matrix elements are known. For instance, and referring to (1)

$$\begin{aligned} t &= \left. \frac{E_2^+}{E_1^+} \right|_{E_2^-=0} = \frac{1}{t_{11}} \\ r &= \left. \frac{E_1^-}{E_1^+} \right|_{E_2^-=0} = \frac{t_{21}}{t_{11}}. \end{aligned} \quad (3)$$

On the other hand, the transmission matrix is widely used in microwave engineering, especially in the solution of transmission line problems, but it is practically unknown by the photonics engineer. Nevertheless, it can be employed for the analysis of photonic devices. The transmission matrix relates the transverse tangential electric (V) and magnetic (I) fields perpendicular to the propagation axis at the left and right part of the device. Referring to the upper part of Fig. 2, the following fields are defined:

$$\begin{aligned} V_i &= E_i^+ + E_i^- \\ I_i &= \frac{1}{Z_i}(E_i^+ - E_i^-) \\ i &= 1, 2 \end{aligned} \quad (4)$$

where Z_i represents the impedance of medium i. For plane waves $Z_i = Z_o/n_i = 120\pi/n_i$, where n_i is the refractive index of the medium. Then the transmission matrix for the device is defined as follows:

$$\begin{pmatrix} V_1 \\ I_1 \end{pmatrix} = \begin{pmatrix} A & B \\ C & D \end{pmatrix} \cdot \begin{pmatrix} V_2 \\ I_2 \end{pmatrix} = \|VI\| \cdot \begin{pmatrix} V_2 \\ I_2 \end{pmatrix}. \quad (5)$$

Since both transfer and transmission matrices can be employed to describe the device performance, it is useful to derive the transformation relationships between them. Using (1), (4), and (5). one finds

$$\begin{aligned} A &= \frac{t_{11} + t_{12} + t_{21} + t_{22}}{2} \\ B &= \left(\frac{t_{11} - t_{12} + t_{21} - t_{22}}{2} \right) Z_2 \\ C &= \frac{t_{11} + t_{12} - t_{21} - t_{22}}{2Z_1} \\ D &= \left(\frac{t_{11} - t_{12} - t_{21} + t_{22}}{2Z_1} \right) Z_2 \end{aligned} \quad (6)$$

And:

$$t_{11}=\frac{1}{2}\left[A+\frac{B}{Z_2}+CZ_1+\frac{DZ_1}{Z_2}\right]$$
$$t_{12}=\frac{1}{2}\left[A-\frac{B}{Z_2}+CZ_1-\frac{DZ_1}{Z_2}\right]$$
$$t_{21}=\frac{1}{2}\left[A+\frac{B}{Z_2}-CZ_1-\frac{DZ_1}{Z_2}\right]$$
$$t_{22}=\frac{1}{2}\left[A-\frac{B}{Z_2}-CZ_1+\frac{DZ_1}{Z_2}\right]. \tag{7}$$

A cascade rule for transmission matrices can also be derived, which states that the overall transmission matrix of a cascade of N elements is the product of the transmission matrices of each element taken form the leftmost to the rightmost element. Referring to the lower part of Fig. 2

$$\begin{aligned}\begin{pmatrix}V_1\\I_1\end{pmatrix}&=\begin{pmatrix}A^{(1)}&B^{(1)}\\C^{(1)}&D^{(1)}\end{pmatrix}\cdot\begin{pmatrix}V_2\\I_2\end{pmatrix}\\&=\begin{pmatrix}A^{(1)}&B^{(1)}\\C^{(1)}&D^{(1)}\end{pmatrix}\begin{pmatrix}A^{(2)}&B^{(2)}\\C^{(2)}&D^{(2)}\end{pmatrix}\cdot\begin{pmatrix}V_3\\I_3\end{pmatrix}=\cdots\\&=\begin{pmatrix}A^{(1)}&B^{(1)}\\C^{(1)}&D^{(1)}\end{pmatrix}\begin{pmatrix}A^{(2)}&B^{(2)}\\C^{(2)}&D^{(2)}\end{pmatrix}\cdots\\&\quad\begin{pmatrix}A^{(N)}&B^{(N)}\\C^{(N)}&D^{(N)}\end{pmatrix}\begin{pmatrix}V_{N+1}\\I_{N+1}\end{pmatrix}\\&=\left[\prod_{j=1}^{N}||VI_j||\right]\cdot\begin{pmatrix}V_{N+1}\\I_{N+1}\end{pmatrix}.\end{aligned} \tag{8}$$

Once the overall transmission matrix of a device is known, its field reflection and transmission transfer functions are given by (3), (7)

$$t=\frac{2}{\left[A+\frac{B}{Z_2}+CZ_1+\frac{DZ_1}{Z_2}\right]}$$
$$r=\frac{\left[A+\frac{B}{Z_2}-CZ_1-\frac{DZ_1}{Z_2}\right]}{\left[A+\frac{B}{Z_2}+CZ_1+\frac{DZ_1}{Z_2}\right]}. \tag{9}$$

B. Transmission Matrices of Some Simple Elements

Fig. 3 shows three basic elements for the construction of complex photonic structures. The upper part shows an interface between two dielectrics with refractive indexes given by n_1 and n_2; the middle structure represents a dielectric with refractive index n and length L; and the lower structure is the cascade of the prior two. We will assume normal incidence. To derive the transmission matrices of the first two elements, we will use their transfer matrices, which are well known and apply the transformations given by (6).

In the case of the transition between two dielectrics, its transfer matrix is given by [3]

$$||T_t||=\begin{pmatrix}t_{11}&t_{12}\\t_{21}&t_{22}\end{pmatrix}=\frac{1}{\tau_{12}}\begin{pmatrix}1&\rho_{12}\\\rho_{12}&1\end{pmatrix}$$
$$\tau_{12}=\frac{2n_1}{n_1+n_2}$$
$$\rho_{12}=\frac{n_1-n_2}{n_1+n_2}. \tag{10}$$

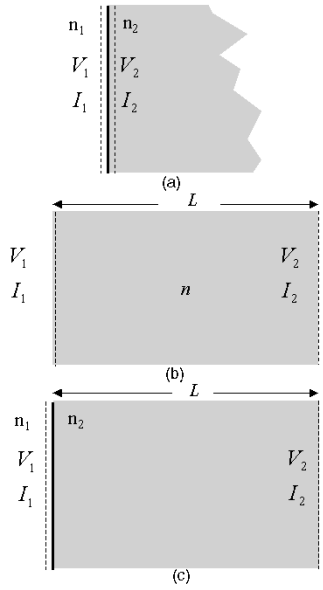

Fig. 3. Three basic elements for the construction of complex photonic structures. (a) Interface between two dielectrics with refractive indexes given by n_1 and n_2, (b) dielectric with refractive index n and length L, and (c) cascade of the prior two.

Using (6), we get

$$||VI_t||=\begin{pmatrix}A&B\\B&C\end{pmatrix}=\begin{pmatrix}1&0\\0&1\end{pmatrix}. \tag{11}$$

This important property states that the transmission matrix of a dielectric transition is the unity matrix.

For the propagation through a lossless dielectric with refractive index n and length L, the transfer matrix is given by

$$||T_p||=\begin{pmatrix}t_{11}&t_{12}\\t_{21}&t_{22}\end{pmatrix}=\begin{pmatrix}e^{j\phi}&0\\0&e^{-j\phi}\end{pmatrix}$$
$$\phi=\frac{2\pi n}{\lambda}L. \tag{12}$$

Again, using (6), we directly get

$$||VI_p||=\begin{pmatrix}A&B\\B&C\end{pmatrix}=\begin{pmatrix}\cos\phi&jZ\sin\phi\\j\frac{\sin\phi}{Z}&\cos\phi\end{pmatrix}$$
$$Z=\frac{120\pi}{n}. \tag{13}$$

The reader can now check by using (8), (11), and (13) that the overall transmission matrix of the cascade structure (lower part of Fig. 3) is exactly equal to that given by (13). This means that whereas for characterizing this structure using transfer matrices we need to multiply three individual transfer matrices, only one matrix is needed if we employ the transmission matrix formalism. This points out the possibility of saving matrix operations when using the latter approach to characterize complex photonic devices composed of dielectric transitions. We will elaborate on this in the next section.

III. The V-I Method for the Analysis of Photonic Components: Application to Fiber Bragg Gratings

We briefly discuss the applicability of the V–I method to the analysis of photonic devices presenting some general considerations. We then develop this method for the analysis of arbitrary fiber and integrated Bragg Gratings.

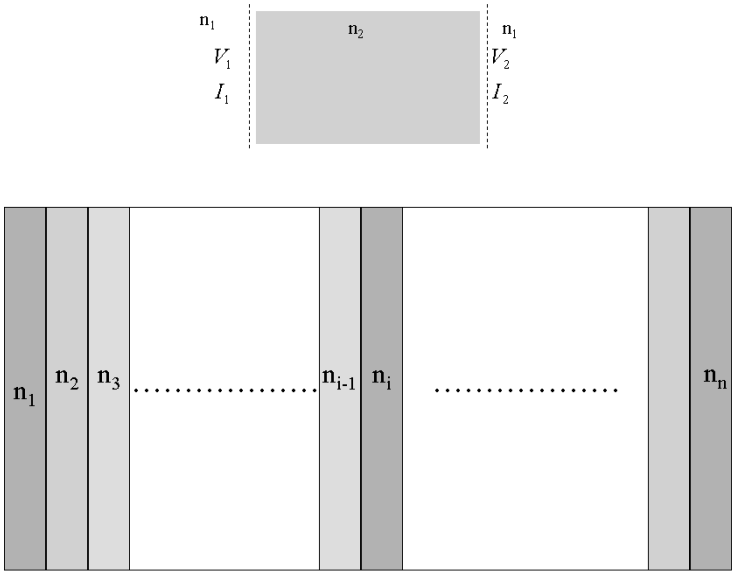

Fig. 4. (a) Fabry–Perot cavity composed of an intermediate dielectric n_2 and length L surrounded by a dielectric with refractive index n_1. (b) Device composed of a stack of n dielectrics.

A. General Considerations

Our previous discussion has pointed out the possibility of saving matrix operations by employing the transmission matrix approach (V–I method from now on) rather than the transfer matrix approach. The V–I method is advantageous if we need to analyze complex photonic devices built from the cascade of dielectric layers. Many photonic devices fall under this category, including dielectric etalons, Fabry–Perot etalons, multilayer thin-film filters, distributed Bragg filter lasers, and fiber and integrated Bragg gratings. Fig. 4 shows two specific examples that we will employ to illustrate this advantage. The upper part of Fig. 4 shows a Fabry–Perot cavity composed of an intermediate dielectric layer with refractive index n_2 and length L surrounded by a dielectric with refractive index n_1. Using the results derived in Section II-B, its overall V–I matrix is

$$\begin{aligned}\|VI_T\| &= \begin{pmatrix} A & B \\ B & C \end{pmatrix} \\ &= \begin{pmatrix} 1 & 0 \\ 0 & 1 \end{pmatrix} \begin{pmatrix} \cos\phi & jZ_2\sin\phi \\ j\frac{\sin\phi}{Z_2} & \cos\phi \end{pmatrix} \begin{pmatrix} 1 & 0 \\ 0 & 1 \end{pmatrix} \\ &= \begin{pmatrix} \cos\phi & jZ_2\sin\phi \\ j\frac{\sin\phi}{Z_2} & \cos\phi \end{pmatrix} \\ Z_2 &= \frac{120\pi}{n_2}. \end{aligned} \tag{14}$$

Since the V–I matrices of dielectric transitions are always the unity matrix, we can eliminate them when we use the cascade rule (8). Thus, in this case, matrix multiplication is not required, since two of the three matrices are unity. On the other hand, if we were to analyze this structure using the transfer matrix, then

$$\begin{aligned}\|T_T\| &= \begin{pmatrix} t_{11} & t_{12} \\ t_{21} & t_{22} \end{pmatrix} \\ &= \frac{1}{\tau_{12}} \begin{pmatrix} 1 & \rho_{12} \\ \rho_{12} & 1 \end{pmatrix} \begin{pmatrix} e^{j\phi} & 0 \\ 0 & e^{-j\phi} \end{pmatrix} \\ &\quad \times \frac{1}{\tau_{23}} \begin{pmatrix} 1 & \rho_{23} \\ \rho_{23} & 1 \end{pmatrix} \\ \phi &= \frac{2\pi n_2}{\lambda} L \\ \tau_{12} &= \frac{2n_1}{n_1+n_2} \\ \tau_{23} &= \frac{2n_2}{n_1+n_2} \\ \rho_{12} &= -\rho_{23} = \frac{n_1-n_2}{n_1+n_2}. \end{aligned} \tag{15}$$

That is, three matrix operations.

This advantage is greater as the number of dielectric layers increases. For instance, in the lower part of Fig. 4, we show a device composed of a stack of n dielectrics. Proceeding in the same way as for the Fabry–Perot device, we arrive at the conclusion that using the V-I method requires one to calculate a product of N V–I propagation matrices such as those given by (13). Using a transfer matrix approach requires $2N+1$ matrix multiplications (N propagation matrices given by (12) and $N+1$ transition matrices given by (10). The saving is thus given by $N+1$ matrix operations.

B. The V-I Method for the Analysis of Fiber and Integrated Bragg Gratings

1) Analysis of Fiber and Integrated Bragg Gratings: FBGs and integrated Bragg gratings (IBGs) are probably one of the photonic components with more potential applications in current and future wavelength-division multiplexing optical communications systems and networks, including, in particular, microwave photonics and radio-over-fiber systems. The interested reader is referred to the literature [5]–[15] for detailed descriptions of their operation principles and applications.

FBGs and IBGs are produced by applying a spatially varying ultraviolet interference pattern on the core of a photosensitive optical fiber or waveguide, respectively. This creates a z-dependent perturbation of the effective index of the fundamental mode, which is given by [13]

$$n_T(z) = n_{\text{eff}} + \delta n_{\text{eff}}(z)$$
$$\delta n_{\text{eff}}(z) = \delta \bar{n}_{\text{effDC}}(z) + \delta \bar{n}_{\text{effAC}}(z) \cos\left(\frac{2\pi}{\Lambda_o} z + \phi(z)\right). \tag{16}$$

In the above expression, n_{eff} is the effective index of the fundamental mode in the absence of grating and $\delta n_{\text{eff}}(z)$ represents the index perturbation due to the written Bragg grating [13]–[15]. This perturbation is composed of a slow varying average term $\delta_{n\,\text{effDC}}(z)$. A fast varying sinusoidal term with a fixed modulation period given by Λ_o, $\delta_{n\,\text{effAC}}(z)$ is the amplitude of the sinusoidal perturbation, also known as the apodization of the sinusoidal variation, which is also a slowly varying function with z. $\phi(z)$ represents a slowly varying phase term, also known as grating chirp, which is responsible for the local change in the value of the modulation period. The index perturbation described by (16) generates two coupled counterpropagating fundamental modes within the FBG/IBG, which interact between themselves within the perturbation region.

The analysis of a given grating design starts from the knowledge of the perturbation profile as given by (16) and must yield the transmission and reflection transfer functions. The reflection coefficient transfer function shows a bandpass characteristic centered at the Bragg wavelength of the structure, which is given by $\lambda_B = 2n_{\text{eff}}\Lambda_o$. The transmission transfer function on the contrary shows a notch characteristic centered at the Bragg wavelength.

A rich collection of literature [5]–[9] has been produced during the last 25 years devoted to analyzing FBGs and IBGs. Topics include coupled-mode equation (CME) formulations [5], [6], transfer matrix (TM) approaches based on the CME solution of uniform FBG segments [7], and multilayer recursive techniques [8]. Of these, CME and TM methods are the most widely employed since they offer the best tradeoff between exactitude and computational cost. For IBGs, effective index methods (EIMs) [9] based on the multiplication of impedance matching and field propagation matrices that characterize regions comparable to the grating period have been proposed. These methods are exact, but computationally expensive for long corrugation lengths, such as those pertaining to FBGs. We introduce a novel EIM method (V–I method, or VIM) that retains the exactitude but at the same time is computationally comparable to CME. This is achieved in two steps. First, transmission V–I matrices [2] presented in Section II instead of the typical transfer matrices are employed to characterize the signal propagation through the multilayer structure, avoiding the need to compute the impedance-matching matrices and saving half of the required matrix multiplications. Secondly, we show that oversampling (i.e., taking multiple samples of the refractive index variation per period), usually employed to approximate the sinusoidal variation by multiple squared stacks, is not necessary and can be avoided, leading to only two required samples per period.

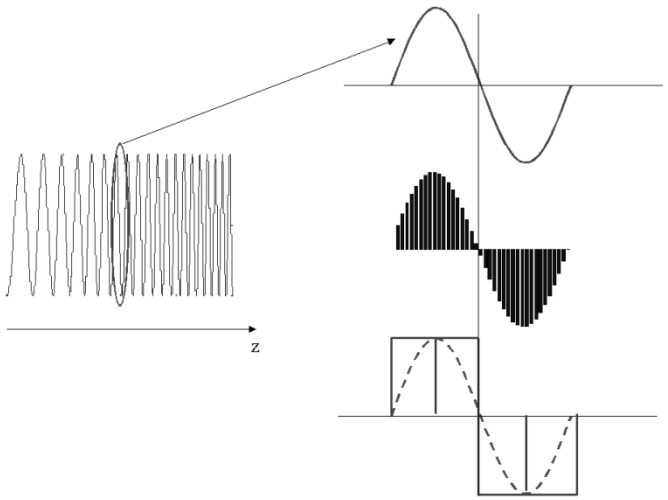

Fig. 5. Oversampling and discretization process of the refractive index profile for an FBG in two steps illustrated for a local period within a linearly chirped uniform FBG (left part and upper and middle traces in the right part). Approximation of the sinusoidal local variation by a periodic square function to eliminate oversampling (right part lower trace).

2) The V-I Method: We refer to the refractive index variation with z in an FBG/IBG given by (16). Effective index matrix methods used to solve the analysis problem proceed first to sample spatially (discretely) the refractive index variation using a spatial discrete sampling step given by Δz. For instance, Fig. 5 shows this sampling process in two steps illustrated for a local period within a linearly chirped uniform FBG. In traditional effective index methods, Δz is much smaller than the local period of the FBG/IBG in order to accurately approximate the sinusoidal variation of the refractive index by the discrete sampling function (see intermediate trace in the right part of Fig. 5). This results in the oversampling of the refractive index profile. For typical applications, the value of the local grating period is around 534 nm, and usually 10–16 samples are taken. This implies that even for short gratings (around 1 cm long), the number of required spatial samples is over 100 000. This figure has to be multiplied by the number of wavelength samples (i.e., the spectral range for which we want to calculate the reflection and transmission transfer functions), which is usually in the range of 500 or higher. These limitations, coupled with the fact that transfer matrices are employed to calculate the field propagation, have prevented the widespread use of the effective index method in the analysis of FBGs.

Our V–I method is based first on the elimination of oversampling while keeping an exact approximation of the refractive

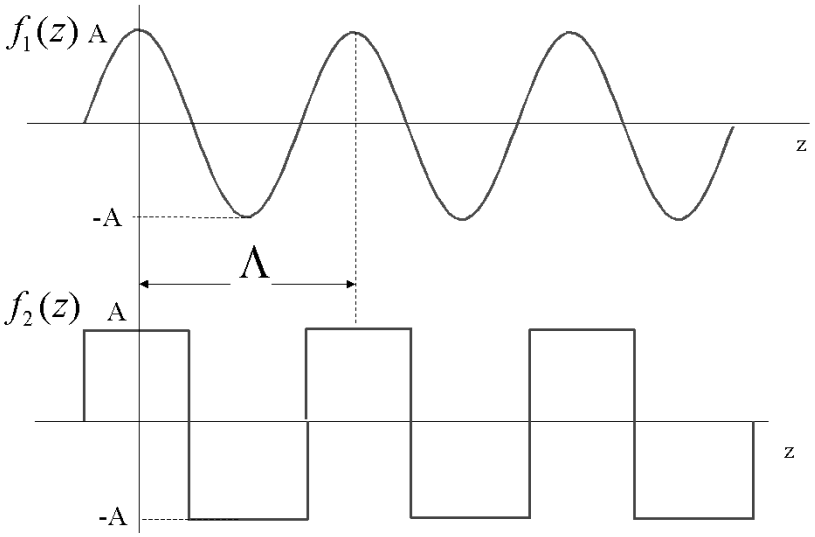

Fig. 6. Approximation of the sinusoidal function $f_1(z)$ by a periodic square function $f_2(z)$.

index profile given by (16), and then by using V–I matrices to compute the propagation though the resulting discrete approximation of the FBG refractive index profile.

To illustrate the elimination of oversampling, the reader is referred to the lower trace in the right part of Fig. 5. Here each local sinusoidal period is approximated by a square function with the same period. The amplitudes of the square function in the positive and negative semiperiods are obtained by taking only two samples; one corresponds to the maximum value (positive semiperiod) and the other corresponds to the minimum value (negative semiperiod). Thus only two samples per period are used in principle in this approximation. The reader could now correctly argue that since this approximation is coarser, it will necessarily yield worse results in terms of accuracy than those obtained using oversampling. In fact, this is true unless a final and fundamental step is taken. Since we are approximating a sinusoidal function by a periodic square function as shown in Fig. 6, we should compare the fundamental term of the Fourier series of the periodic square function with the sinusoidal function that it approximates. Referring to the signals in Fig. 6

$$f_1(z) = A\cos\left[\frac{2\pi}{\Lambda_o}z\right]$$
$$f_2(z) = \frac{4A}{\pi}\cos\left[\frac{2\pi}{\Lambda_o}z\right] + \cdots. \tag{17}$$

A correct approximation requires thus to multiply the amplitude of the periodic square approximation by a factor of $\pi/4$.

The exact location of the sampling points z_m $(\mathrm{m} = 1, 2, 3\ldots)$ along the grating length depends on the FBG/IBG characteristics. For uniform period (i.e., unchirped) gratings $(\phi(z) = \text{constant})$, then, assuming $(\phi(z=0) = 0)$:

$$z_m = \frac{m\Lambda_o}{2}. \tag{18}$$

For chirped gratings, the exact location depends on the chirp profile. For instance, for linearly chirped FBG

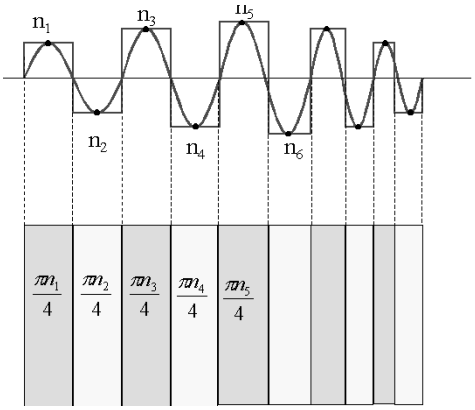

Fig. 7. Ideal location of the spatial sampling points of an aperiodic FBG (upper). Translation of the sampled FBG into a multiplayer dielectric structure for the application of the V-I formalism.

$(\phi(z) = F(z/L)^2)$, where F is the chirp parameter and L is the grating length

$$z_m = \frac{-\frac{L^2}{F}\frac{2\pi}{\Lambda_0} + \sqrt{\left(\frac{L^2}{F}\frac{2\pi}{\Lambda_0}\right)^2 + 4m\pi\frac{L^2}{F}}}{2}. \tag{19}$$

This is illustrated in the upper part of Fig. 7.

The final step is to transform the discretized refractive approximation into a multilayer structure, as shown in the lower part of Fig. 7. The refractive index of each layer is obtained by multiplying the value of the refractive index sample by the normalization constant $\pi/4$. The length of layer m is given by $\Delta z_m = z_m - z_{m-1}$. Once the multilayer structure is obtained, the propagation matrices (13) of each layer have to be calculated and multiplied in the order given by (8). From the overall FBG/IBG transmission matrix, we get the transfer functions using (9), bearing in mind that $Z_1 = Z_2 = 120\pi/n_{\text{eff}}$.

IV. Results and Discussion

The described method has been implemented on a MATLAB+C based platform that includes as well a CME implementation based on a Runge–Kutta RK-23 method

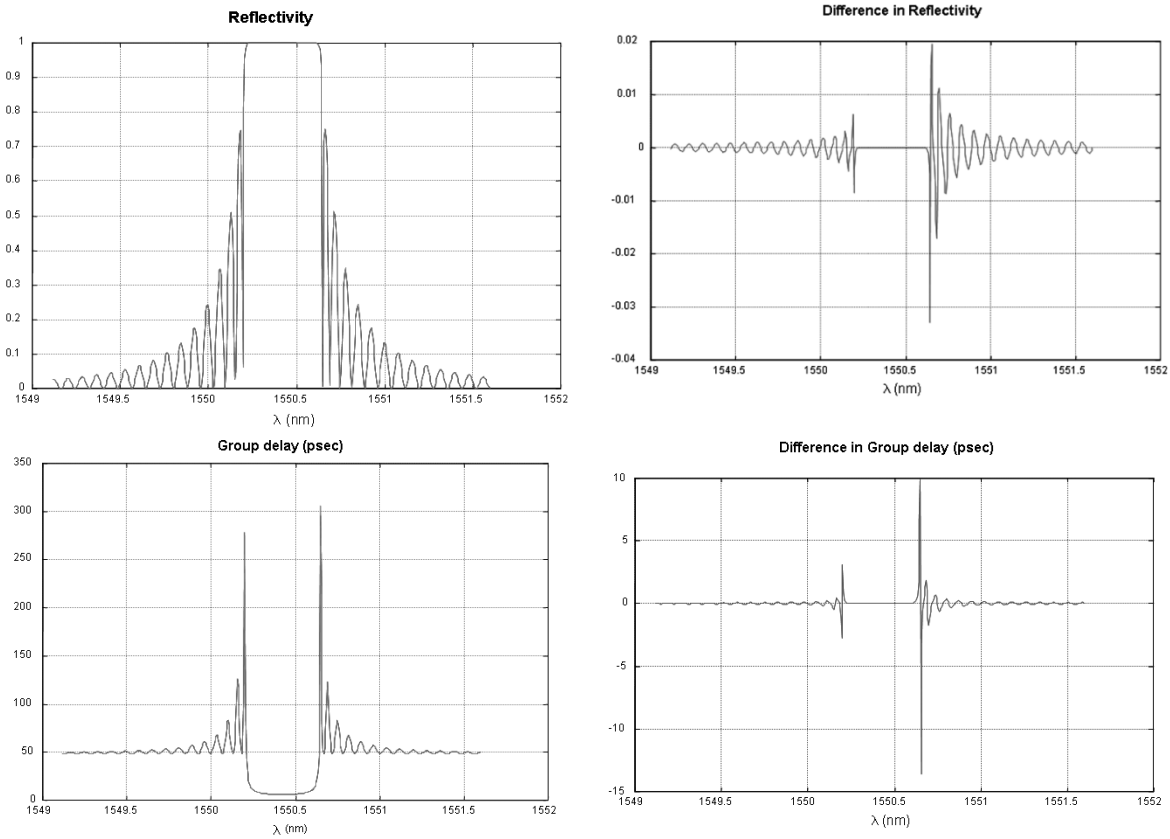

Fig. 8. Modulus and group delay for the reflectivity of a 1-cm-long uniform FBG with $\kappa L = 8$, which corresponds to those obtained in [13, Fig. 7]. Both solutions obtained by the application of the V-I formalism and the solution of CME are plotted. The right part shows the differences between the solutions obtained by using both methods.

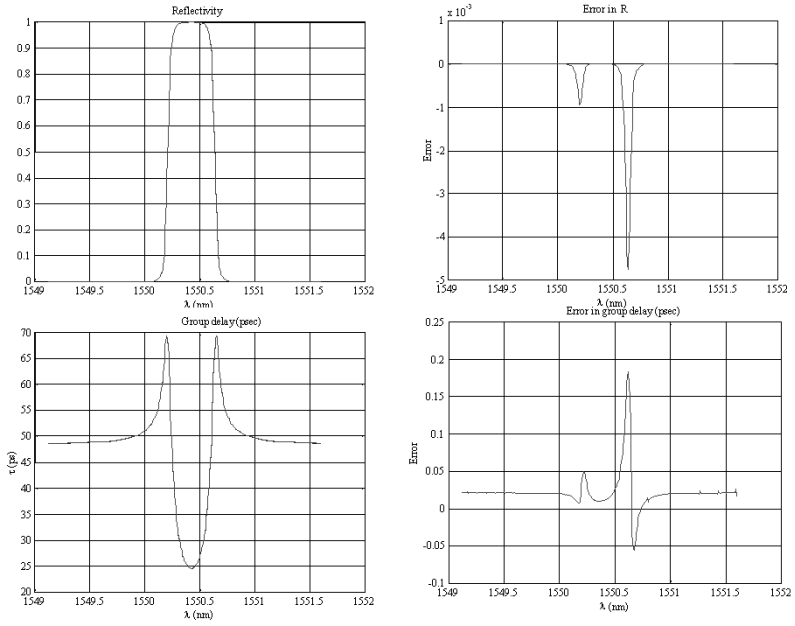

Fig. 9. Similar results as those reported in Fig. 8 for an FBG with uniform period and apodised using a Hanning window [15] with a value for the B parameter [15] of 0.5.

with 10^{-6} precision for comparison. We have tested the V-I formalism proposed in this paper in several ways. First, we have verified that it can be applied to the solution of any kind of FBG/IBG and tested the results with those published by other authors in the literature. Different kinds of FBG profiles have been taken into account including, uniform, apodized, linearly chirped gratings, sinc-sampled gratings, squared sampled gratings, phase-shifted gratings, etc. The results obtained have

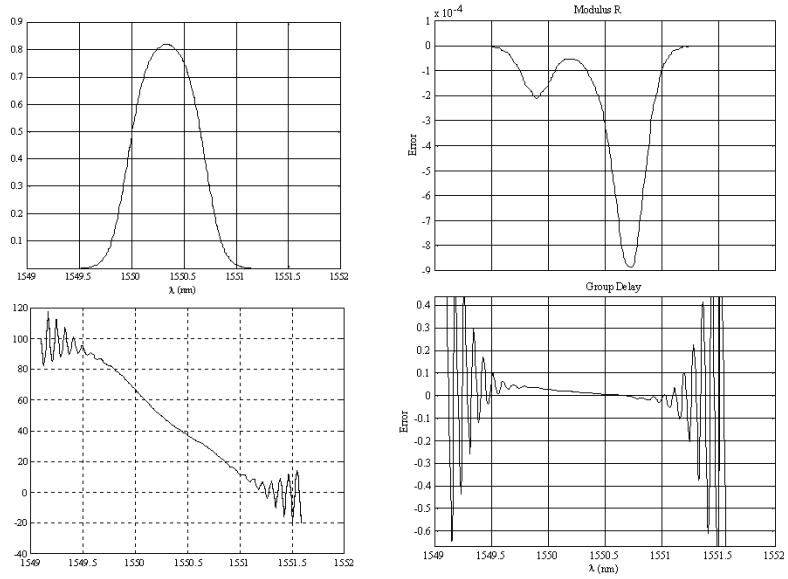

Fig. 10. Results obtained for an example of a linearly chirped Gaussian apodised FBG designed in [14] for dispersion compensator with parameters given by $\kappa L = 2\pi, F = 20\pi, L = 1$ cm and a Gaussian window parameter of $G = 16$ [15]. Both solutions obtained by the application of the V-I formalism and the solution of CME are plotted. The right part shows the differences between the solutions obtained by using both methods.

been identical to those reported elsewhere. Furthermore, the results are extremely similar to those obtained with the CME method, and the computation time almost equivalent. This shows the wide range of applicability of this method.

The left part of Fig. 8 shows the results obtained in modulus and group delay for the reflectivity of a 1-cm-long uniform FBG with $\kappa L = 8$, which corresponds to those obtained in [13, Fig. 7]. The coincidence is exact. Furthermore, both solutions obtained by the application of the V–I formalism and the solution of CME are plotted. It is impossible to distinguish them by pure visual inspection, so the right part shows the differences between the solutions obtained by using both methods. The execution time for a 500-sample wavelength vector was 6 s for both the V–I method and the CME.

Fig. 9 shows similar results for an FBG with uniform period and apodised using a Hanning window [15] with a value for the B parameter [15] of 0.5. The rest of the FBG parameters are similar to those used to compute the results of Fig. 8. Again, the results obtained using the V–I formalism and the CME method are visually undistinguishable. The right part of Fig. 9 shows again the discrepancy in the results. The execution time for a 500–sample wavelength vector was 6 s for the V–I method and 9 s for the CME.

Fig. 10 shows the results for an example of a linearly chirped Gaussian apodised FBG designed in [14] for dispersion compensator with parameters given by $\kappa L = 2\pi, F = 20\pi, L =$ 1 cm and a Gaussian window parameter of $G = 16$ [14], [15]. Here we plot the results for the reflectivity and the group delay obtained by the V–I method and the CME method in the left part and the amplitude and phase difference between both methods in the right part. Again, the coincidence is almost total. The execution time for a 500-sample wavelength vector was 6 s for the V–I method and 12 s for the CME.

The reader can check that in these three examples, the execution time for the V–I method is the same in all the cases

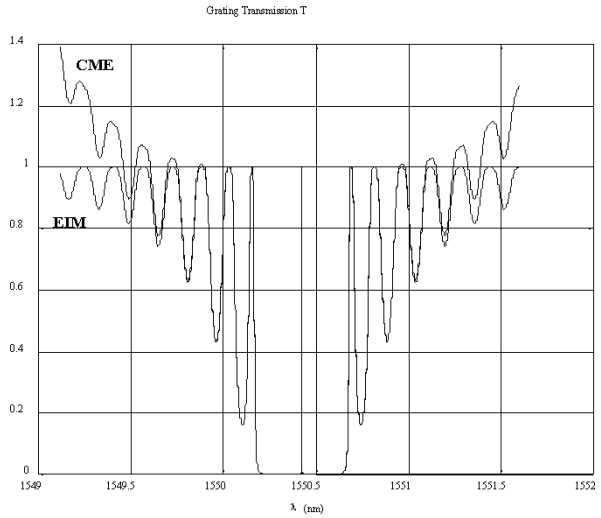

Fig. 11. Results for the transmissivity of a uniform grating with a π phase shift in its center. The grating length is 1 cm, and $\kappa L = 8$. Solution obtained by applying the V-I and CME methods are shown.

regardless of the grating profile. Indeed, in the three cases, the grating length, which fixes the computation time for this method, was identical. On the other hand, the CME computation time is highly dependent on the grating refractive index profile, leading to higher execution times for grating profiles with drastic changes. Furthermore, in these cases, CME might not converge. For instance, in Fig. 11, we plot the results for the transmissivity of an uniform grating with a π phase shift in its center. The grating length is 1 cm, and $\kappa L = 8$. The CME precision had to be reduced to 10^{-4} to achieve convergence with the RK-23 method. The execution times for a 1000-sample wavelength vector were 12 s for the V–I method and 3 s for the CME. However, the reader can appreciate that the CME solution diverges outside the forbidden band, while the V–I method provides a stable solution.

Obtaining a stable solution with the CME requires the use of an integration method (for instance, RK-45) with higher precision and higher computation time.

V. Summary and Conclusion

We have proposed the use of V–I matrices well known in microwave engineering in the analysis of photonic devices, especially those based on multilayer dielectrics. We have shown that using V–I transmission matrices results in a considerable reduction of matrix operations as compared to the case of using transfer matrices. As an application, we have presented a novel fast V–I matrix formalism for the analysis of FBG, which combines the exactitude of traditional impedance-matching effective index methods and the speed of coupled-mode methods. We believe that this method can be extended advantageously as well to other photonic devices, such as those implemented by photonic crystals.

References

[1] A. J. Seeds, "Microwave photonics," *IEEE Microwave Theory Tech.*, vol. 50, pp. 877–887, 2002.

[2] D. M. Pozar, *Microwave Engineering*, 2nd ed. New York: Wiley, 1998.

[3] J. Capmany and M. A. Muriel, "A new transfer matrix for the analysis of fiber ring resonators: Compound coupled structures for FDMA demultiplexing," *IEEE J. Lightwave Technol.*, vol. 8, pp. 1904–1919, 1990.

[4] C. Madsen and J. Zhao, *Optical Filter Design and Analysis: A Signal Processing Approach*. New York: Wiley, 1999.

[5] A. Yariv, "Coupled-mode theory for guided-wave optics," *IEEE J. Quantum Electron.*, vol. QE-9, pp. 919–933, 1973.

[6] H. Kogelnik, "Filter response of nonuniform almost periodic structure," *Bell Syst. Tech. J.*, vol. 55, p. 109, 1976.

[7] M. Yamada and K. Sakuda, "Analysis of almost-periodic distributed feedback slab waveguides via a fundamental matrix approach," *Appl. Opt.*, vol. 26, pp. 3474–3478, 1987.

[8] L. A. Weller-Brophy and D. G. Hall, "Analysis of waveguide gratings: Applications of Rouard's method," *J. Opt. Soc. Amer.*, vol. A-4, pp. 60–65, 1987.

[9] K. A. Winick, "Effective-index method and coupled-mode theory for almost-periodic waveguide gratings: A comparison," *Appl. Opt.*, vol. 31, pp. 757–764, 1992.

[10] K. O. Hill and G. Meltz, "Fiber Bragg grating technology fundamentals and overview," *J. Lightwave Technol.*, vol. 15, no. 8, pp. 1263–1276, 1997.

[11] R. Kashyap, *Fiber Bragg Gratings*. San Diego, CA: Academic, 1999.

[12] A. Othonos and K. Kalli, *Fiber Bragg Gratings: Fundamentals and Applications in Telecommunications and Sensing*. Boston, MA: Artech House, 1999.

[13] T. Erdogan, "Fiber grating spectra," *J. Lightwave Technol.*, vol. 15, pp. 1277–1294, 1997.

[14] F. Ouellete, "Dispersion cancellation using linearly chirped Bragg grating filters in optical waveguides," *Opt. Lett.*, vol. 12, pp. 847–849, 1987.

[15] D. Pastor *et al.*, "Design of apodised linearly chirped fiber Bragg gratings for dispersion compensation," *J. Lightwave Technol.*, vol. 14, pp. 2581–2588, 1996.

José Capmany (S'88–M'91–SM'96) was born in Madrid, Spain, on December 15, 1962. He received the telecommunications engineer and Ph.D. degrees from the Universidad Politécnica de Madrid, Madrid, Spain, in 1987 and 1991, respectively.

From 1988 to 1991, he worked as a Research Assistant at the Departamento de Tecnología Fotónica, Universidad Politécnica de Madrid. In 1991, he moved to the Departamento de Comunicaciones, Universidad Politécnica de Valencia, Valencia, Spain, where he initiated activities related to optical communications and photonics, founding the Optical Communications Group (www.gco.upv.es). He was an Associate Professor from 1992 to 1996 and Full Professor in optical communications, systems, and networks since 1996. At the same time, he was Telecommunications Engineering Faculty Vice-Dean from 1991 to 1996 and has been deputy head of the Communications Department since 1996. In 2002, he was appointed as the Director of the Institute of Informatics, Multimedia, Communications and Computers (IMCO2) of the Universidad Politécnica de Valencia, which now has more than 140 researchers focusing on research in information technologies and applications. His research activities and interests cover a wide range of subjects related to optical communications, including optical signal processing; microwave photonics; fiber radio systems; fiber resonators; fiber gratings; radio frequency (RF) filters; subcarrier-multiplexing (SCM), wavelength-division-multiplexing (WDM), and CDMA transmission; wavelength conversion; and optical bistability. He has published more than 170 papers in international refereed journals and conferences, five textbooks on optical communications, and three chapters in international research books. He has been a reviewer for 25 international scientific journals in the field of optics, photonics, and optical communications, and he also is or has been a Member of the editorial board of *Fiber and Integrated Optics*, *Microwave and Optical Technology Letters*, *Optical Fiber Technology*, and the *International Journal of Optoelectronics*. He has been leader of more than 15 national or international research projects, and he is currently the leader of the European Union-funded IST project LABELS, dealing with the implementation of optical internetworks based on subcarrier multiplexed label swapping.

Dr. Capmany is a Fellow of the Optical Society of America (OSA) and is or has been a Member of the Technical Programme Committees of the European Conference on Optical Communications (ECOC), the Optical Fiber Conference (OFC), the Integrated Optics and Optical Communications Conference (IOOC), CLEO Europe, and the Optoelectronics and Communications Conference (OECC). He has also conducted activities related to professional bodies and is the Founder and current Chairman of the IEEE Lasers and Electro-Optics Society (LEOS) Spanish Chapter and a Fellow of the Institution of Electrical Engineers (IEE). He was the recipient of the extraordinary doctorate prize of the Universidad Politécnica de Madrid in 1992 and has been a Guest Editor for the IEEE Journal on Selected Topics in Quantum Electronics.

Miguel A. Muriel (M'84–SM'98) was born in Burgos, Spain, on October 19, 1955. He received the Ingeniero de Telecomunicación (M.S.) and Doctor Ingeniero de Telecomunicación (Ph.D.) degrees (*summa cum laude*) from the E.T.S. Ingenieros de Telecomunicación, Universidad Politécnica de Madrid, Spain, in 1978 and 1980, respectively.

He has been with E.T.S. Ingenieros de Telecomunicación since 1979, as Assistant Professor (1980), Associate Professor (1983), and Full Professor (1989), and he was the Head of the Photonic Technology Department from 1989 to 1997. He has published more than 120 international papers and conference contributions, in the fields of liquid crystals, optical bistability, optical chaos, pulse propagation in fibers and optical structures, optical signal processing, integrated optics, fiber-optic structures for signal processing, linear and nonlinear resonators, fiber-optics sensors, fiber Bragg gratings, time–frequency analysis, time–space duality, spectral analysis, and wavelength-division multiplexing. He has led 12 research engineering projects, some of them with Spanish and European industries. He has taught courses on optical electronics, optical communications, Fourier optics, electrooptical devices, lasers, and optical signal processing. He has also acted as technical reviewer for several journals in the field of optoelectronics and optical communications. His professional interests cover fiber gratings, periodic structures, time–frequency representations, time–space duality and in general signal processing applied to photonics, antennas and wireless communications.

Prof. Muriel is a Member of the Optical Society of America (OSA). He has received awards for the best doctoral dissertation from the Universidad Menendez y Pelayo, Universidad Politécnica de Madrid, and Colegio de Ingenieros de Telecomunicación. In addition, he has received the Junior Research Award of the Universidad Politécnica de Madrid in 1989 and the Senior Research Award of the Universidad Politécnica de Madrid in 1998.

Salvador Sales (S–91–M'96–SM'03) was born in Valencia, Spain, in 1969. He received the telecommunications engineer and the Ingeniero Superior de Telecomunicación degrees and the Ph.D. degree in communications from the Universidad Politécnica de Valencia, Valencia, Spain, in 1990, 1992, and 1995, respectively.

He joined the Departamento de Comunicaciones, Universidad Politécnica de Valencia (UPV), Valencia, Spain, in 1993, where he was a Research Assistant and, subsequently, a Lecturer with the Optical Communications Group. Since 1997, he has been an Associate Professor with the Departamento de Comunicaciones, UPV. He was also Faculty Vicedean of UPV in 1998. In 1999, he joined the Optoelectronics Research Center, University of Southampton, Southampton, U.K., for a short-term mission. He is coauthor of more than 40 journal papers and international conferences. He has been collaborating and leading some national and European research projects since 1997. His main research interests include optoelectronic signal processing for optronic and microwave systems, optical delay-line filters, fiber Bragg gratings, wavelength-division-multiplexing (WDM) and subcarrier multiplexing (SCM) lightwave systems and semiconductor optical amplifiers.

Dr. Sales received the Annual Award of the Spanish Telecommunication Engineering Asociation for the best Ph.D. dissertation on optical communications. He has also served as a Reviewer for the IEEE and IEE journals since 1995. He has been a Member of the IEEE Laser and Electro-Optic Society (LEOS) since 1991.

Juan José Rubio was born in Valencia, Spain, in 1978. He received the M.S. degree in telecommunications engineering in 2003.

He is currently a Consultant and Programmer.

Daniel Pastor (M'96) was born in Elda, Spain, on November 5, 1969. He received the telecommunications engineer and Ph.D. degrees from the Universidad Politécnica de Valencia, Valencia, Spain, in 1993 and 1996, respectively.

He joined the Optical Communications Group of the Departamento de Comunicaciones, the Universidad Politécnica de Valencia, in 1993. From 1994 to 1998, he was a Lecturer with the Telecommunications Engineering Faculty and became an Associate Professor in 1999. He has been involved in different research activities related to optical communications and optical signal processing, such as optical delay-line filters, fiber Bragg gratings, microwave photonics, wavelength-division-multiplexing (WDM) and subcarrier-multiplexing (SCM) lightwave systems and optical networks.